

# Supplemental Figures

## Supplemental Items:

### 1. Supplemental Figure Legends:

- Figure S1 (related to Figure 1) shows the *C9orf72* BAC repeat stability seen in bacteria, and after BAC integration into the mouse genome.
- Figure S2 (related to Figure 2 and 3) shows p62, TDP43, and ubiquitin staining in the brain and spinal cord of C9-BACexp mice (line F112) compared to nontransgenic controls at 13.5 months. Immunostaining at of microglia (anti-IBA1, astrocytes (anti-GFAP), neurons (anti-NeuN), and synapses (anti-synaptophysin) in 20 month old mice in different brain regions and spinal cord.
- Figure S3 (related to Figure 4) shows costaining of sense and antisense RNA Foci with hnRNP A2/B1, hnRNP A3, hnRNP H, and pur- $\alpha$  in C9-BACexp (F112). Splicing of RAN GTPase and ribosomal RNA processing in C9-BACexp (F112) compared to nontransgenic controls at 8 months.
- Figure S4 shows a summary of RNA-Seq analysis performed on cortical tissue from C9-BACexp (F112), F08-CTR and nontransgenic control mice at 6 month of age.

Figure S1

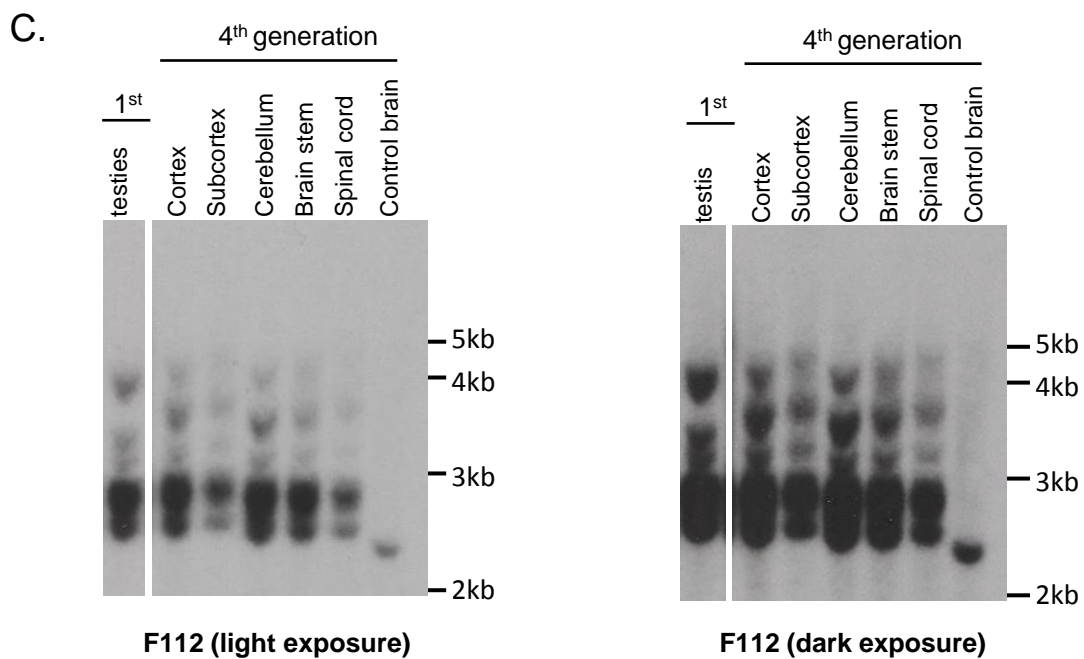
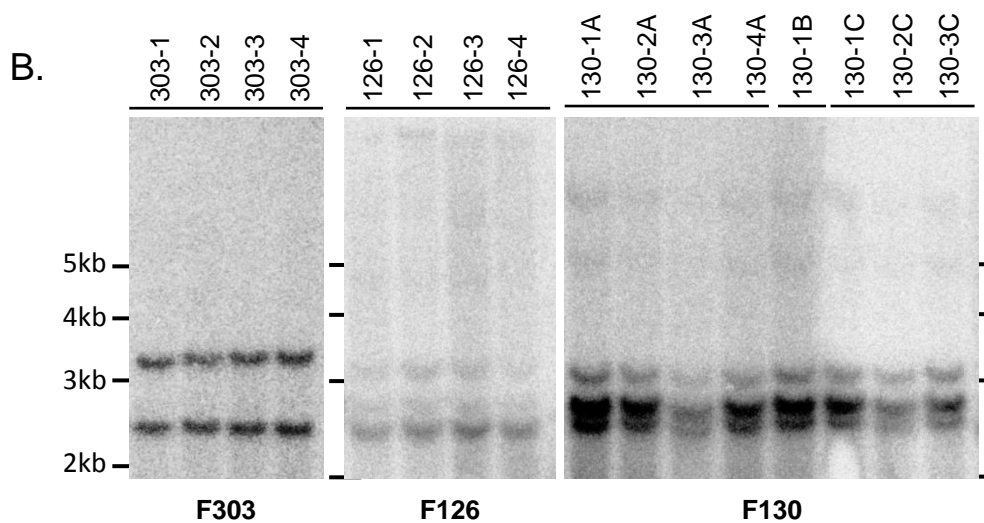
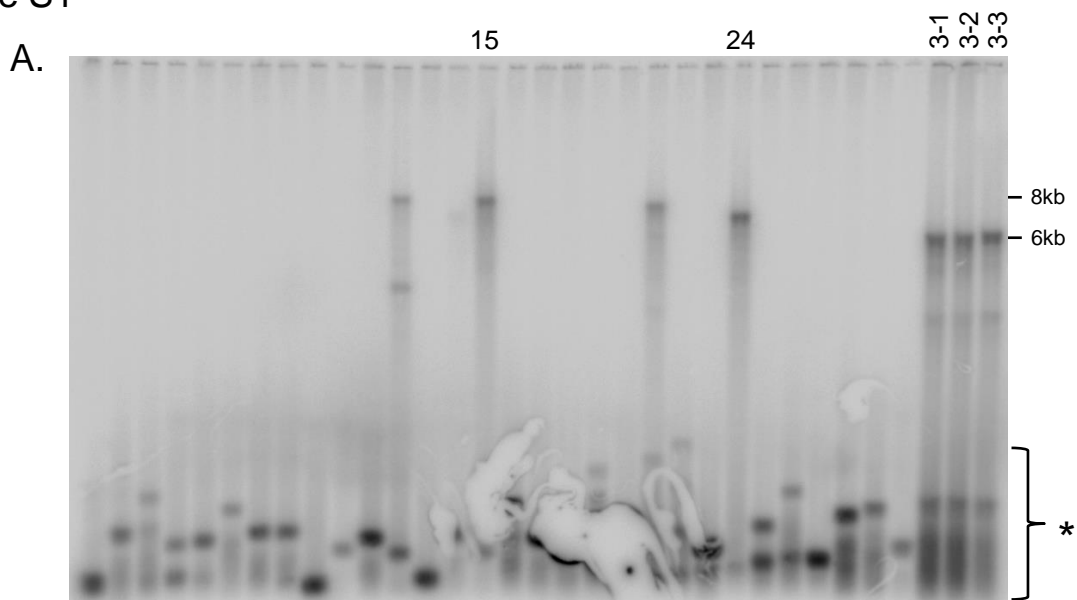


Figure S1 (related to Figure 1): *C9orf72* BAC stability in bacteria and after integration into the mouse genome.

A) The GGGGCC repeat is highly unstable in bacteria. Southern blot analysis of individual subclones isolated from BAC 239 containing human *C9orf72* with the GGGGCC expansion. Subclones #3, #15, and #24 were used to generate C9-BACexp mice, and subclone #3 was used to generate lines F112 and F113. (\*) Asterisk demonstrates subset of partially contracted repeat containing BACs present in most BAC preps. B) Southern blot analysis showing transgene stability across littermate progeny for 3 different lines - F303, F126, and F130, and A, B, C represent 3 different litters for F130. No differential segregation of bands or repeat instability was observed. C) Repeat stability across generations and tissues. Southern blot comparing repeat sizes from testis of a 1<sup>st</sup> generation F112 mouse with brain regions from a 4<sup>th</sup> generation back-crossed F112 mouse. After multiple back-crosses to C57B6 no significant differences in banding patterns were observed either from earlier generations, or across different brain regions.

Figure S2

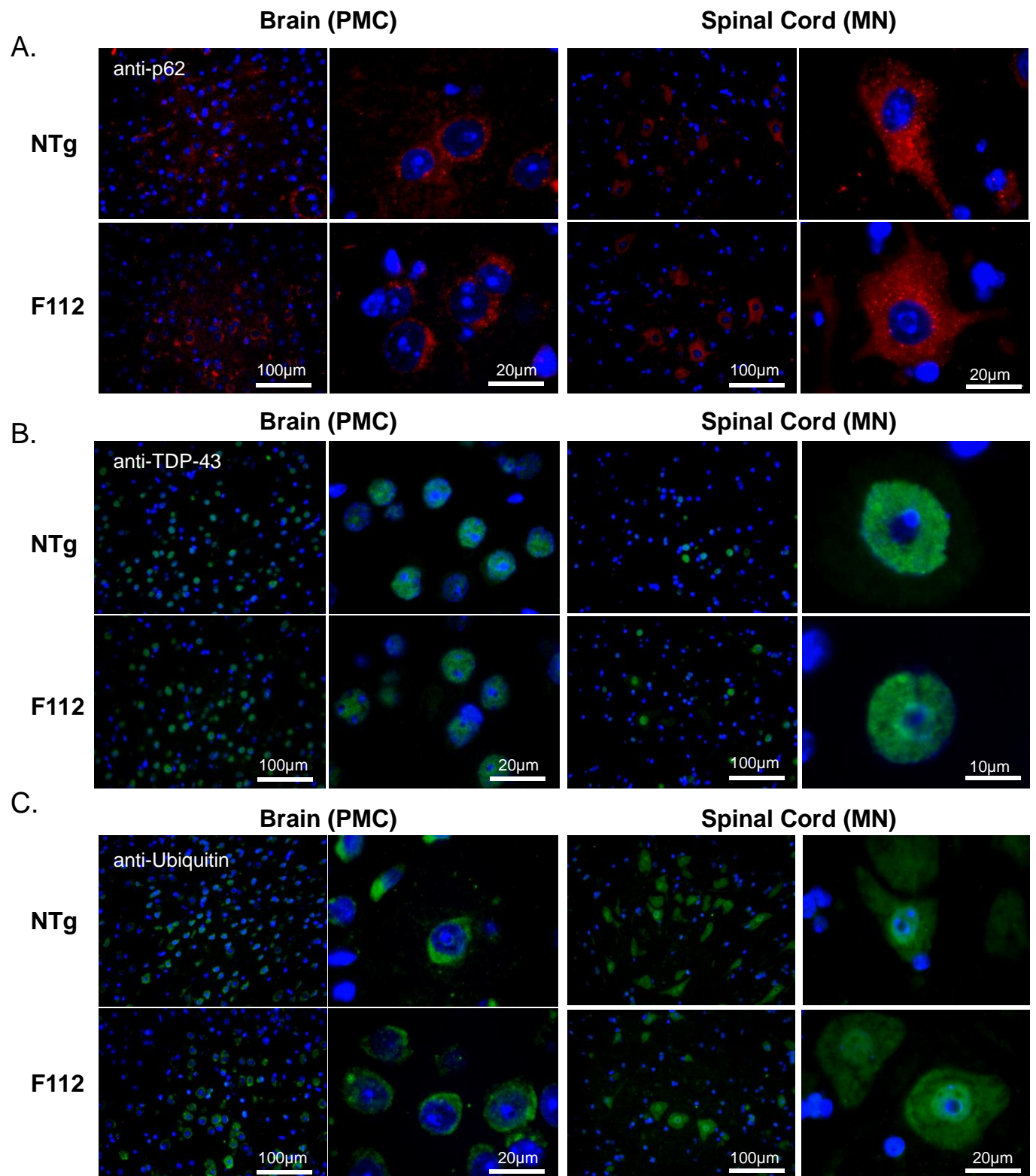


Figure S2 cont.

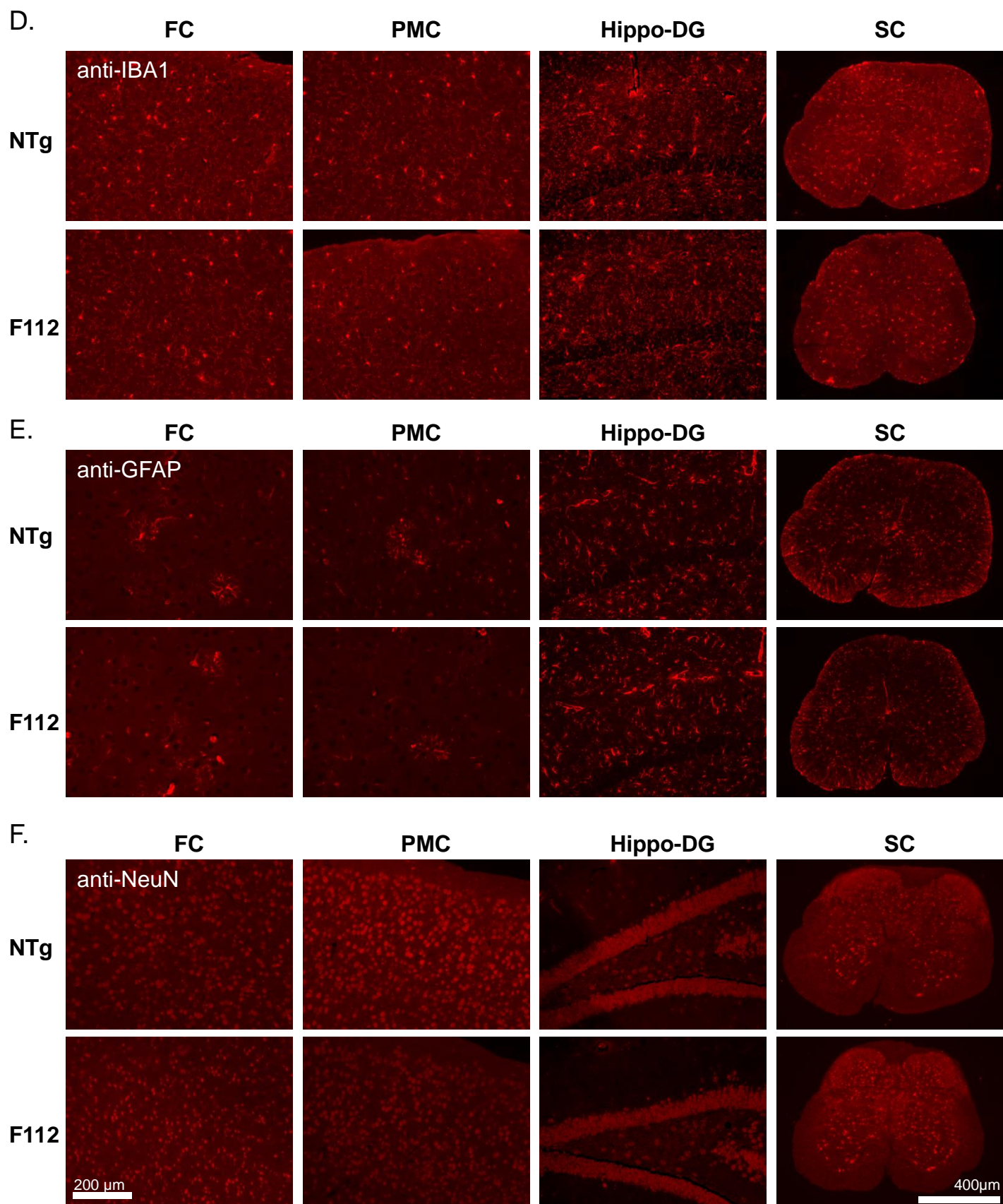


Figure S2 cont.

G.

FC

PMC

Hippo-DG

SC

anti-SYN

NTg

F112

200  $\mu$ m

400  $\mu$ m

H.

Hippo-DG

Hippo-CA1

anti-SYN

NTg

F112

20  $\mu$ m

Figure S2 (related to Figures 2 and 3): Pathogenic inclusions are not observed in C9-BACexp mice (F112).

A) Representative p62 images in aged C9-BACexp mice. No differences in p62 staining detected in brain (primary motor cortex, PMC) or spinal cord (SC) when comparing C9-BACexp (F112) and nontransgenic controls (NTg) at 13.5 months. scale bar = 100 $\mu$ m for 20x images (left), 20 $\mu$ m for 100x images (right). B) Representative TDP-43 images in aged C9-BACexp mice. No differences in TDP-43 staining observed in brain (primary motor cortex, PMC) or spinal cord (SC) between C9-BACexp (F112) and nontransgenic controls (NTg) at 13.5 months. scale bar = 100 $\mu$ m for 20x images (left), 10 $\mu$ m for 100x images (right). C) Representative ubiquitin images in aged C9-BACexp mice. No differences detected in ubiquitin staining when comparing C9-BACexp (F112) mice to nontransgenic control (NTg) brain (primary motor cortex, PMC) and spinal cord (SC) at 13.5 months. scale bar = 100 $\mu$ m for 20x images (left), 20 $\mu$ m for 100x images (right). D) Immunohistochemical evaluation of microglia (D, IBA1), astrocytes (E, GFAP), neurons (F, NeuN), and synapses (G, Synaptophysin (SYN)) in the frontal cortex (FC), primary motor cortex (PMC), hippocampus dentate gyrus region (Hippo-DG), and spinal cord (SC) of C9BACexp (F112) and nontransgenic (NTg) mice at 20 months of age. H) Higher magnification (100x) of synpatophysin (SYN) staining in the hippocampus dentate gyrus and CA-1. C9BACexp carrying the expanded GGGGCC are indistinguishable from age matched nontransgenic controls.





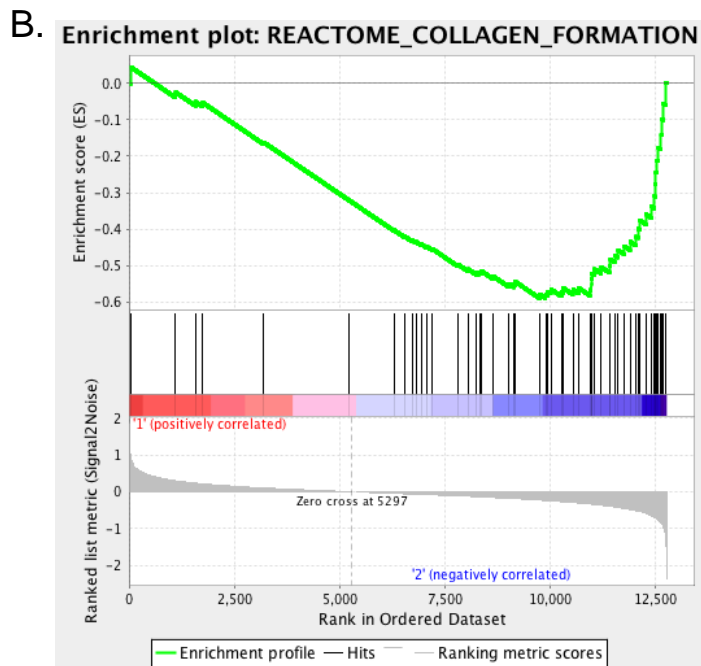
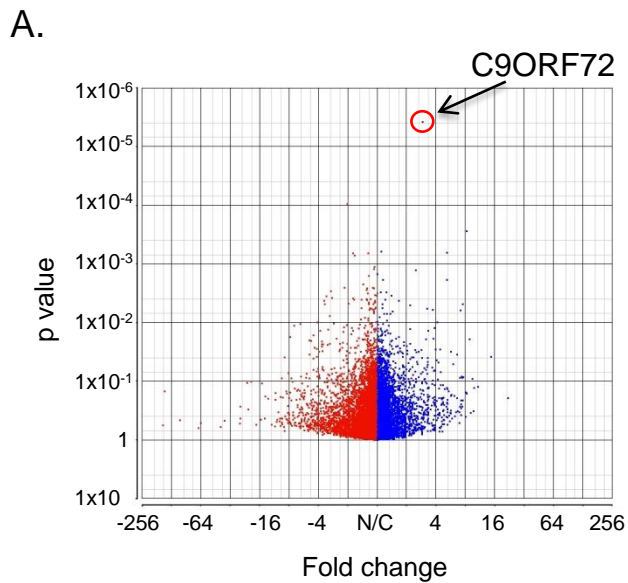
Figure S3 (related to Figure 4): Sequestration of RNA binding proteins are not observed in C9-BACexp mice (F112).

A) Co-staining of FISH for sense and antisense foci with immunofluorescence for RNA binding proteins (RBP). Minimal costaining and no sequestration of hnRNP A2/B1, Pur- $\alpha$ , hnRNP A3 or hnRNP H was observed with either sense or antisense foci in the brains of C9-BAC mice. (scale bar = 10 $\mu$ m).

B) Normal RAN GTPase splicing observed in C9-BACexp mice (F112). Assessment of exon 2 skipping for RAN GTPase (from Kwon et al., Science, 2014), showed no abnormality in splicing when comparing C9-BACexp mice (n=3) to nontransgenic (NTg) controls (n=3) at 8 months of age.

C and D) Maturation of ribosomal RNA (45S) in C9-BACexp mice at 8 months. qPCR showing 45S pre-rRNA processing to 18S, 5.8S, and 28S in nontransgenic (NTg, n=3) compared to C9-BACexp (F112, n=3), normalized to actin (C) and total 45S (D). 18S is slightly decreased in F112 mice, but this is not significant (t-test, p-value = 0.07265 and 0.0819, respectively) and no differences were detected for 5.8S or 28S at 8 months.

Figure S4



C.

Gene Set	Size	Normalized Enrichment Score	FDR q-value
REACTOME COLLAGEN FORMATION	56	-1.9481	0.0221
BIOCARTA DC PATHWAY	20	-1.8336	0.0377
BIOCARTA CTLA4 PATHWAY	16	-1.8149	0.0395
REACTOME TIGHT JUNCTION INTERACTIONS	29	-1.8053	0.0405
BIOCARTA GATA3 PATHWAY	15	-1.7912	0.0424
KEGG PRIMARY IMMUNODEFICIENCY	32	-1.7938	0.0424
KEGG CYTOSOLIC DNA SENSING PATHWAY	40	-1.7824	0.0448
BIOCARTA TNFR2 PATHWAY	18	-1.7656	0.0498

D.

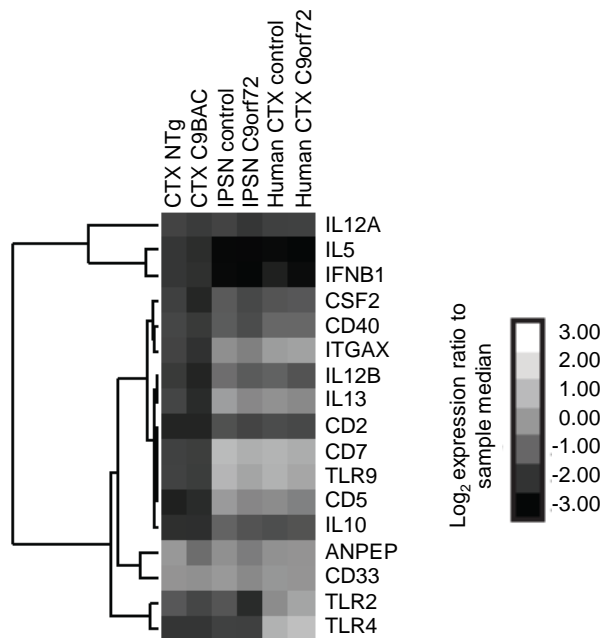


## Figure S4: Summary of RNA-seq analysis in C9-BAC transgenic mice

A) Volcano plot of differentially expressed genes (C9-BACexp F112 vs. nontransgenic control). Similar results were obtained from C9-BAC F08-CTR vs. nontransgenic, and C9-BAC F112 vs F08-CTR.

B) Gene set enrichment analysis (GSEA) plot for top differentially expressed category (Collagen Formation). Transcriptional profiles of C9-BACexp cortex (n=3) were compared to NTg (n=4) cortex at 6 months of age. Genes along the x-axis heatmap were ranked using the signal-to-noise metric, where red indicates relative high expression in C9-BACexp, and blue indicates relative high expression in nontransgenic. This ranked list was then tested against the MSigDB database for enrichment of BIOCARTA, KEGG, and REACTOME pathway gene sets. Significantly enriched pathway gene sets (FDR q-value < 0.05) are listed in the table below (C).

D) Heat map for each of the genes defining the dendritic cell (DC) pathway regulating TH1 and TH2 cell development , which was downregulated in both C9-BACexp mouse cortex and C9orf72 human iPSC derived neurons.

## **Supplemental Experimental Procedures**

*BAC Isolation and Characterization:* Amplicon Express generated a BAC library from genomic DNA obtained from skin fibroblasts from an ALS patient (28i from (Sareen et al., 2013)). The 174 kb pCC1-BAC contained 166 kb of the human *C9orf72* locus along with the GGGGCC repeat expansion as determined by repeat primed PCR. Of 36,864 colonies screened, 7 contained the entire *C9orf72* genomic region, and 1 contained the expanded allele (BAC clone 239). BAC clones were propagated using Electromax DH10B T1 cells (Cat # 12033-015), and each subclone was screened using Southern blot analysis. A subclone which contracted down to 15 repeats was used to generate the F08-CTR line.

*Mouse production and breeding:* Subclones of BAC 239 were microinjected into C57BL/6J blastocysts to generate 30 C9-BAC transgenic founders. Lines F112, F113 and F08 were chosen for further characterization based on repeat size and expression levels. Transgene insertion was confirmed using genomic DNA prepared from tail using alkaline lysis. Primers designed to both the 5' end and 3' end of the BAC construct were used to PCR amplify the C9-BAC. 5' end (Forward primer 5'-CAGACGTAACCTACGGTGTCC-3' and Reverse primer-5'-CGACTCCTGAGTTCCAGAGC-3') and 3' end (Forward: 5'- TGTTTGCCTGCAATAGGC-3' and Reverse: 5'- TGATGGGAAAGCTATTATGACC-3'). F112 and F113 were generated from subclone #3 and C9-BAC mice were maintained on the C57BL/6J background.

*Antibodies, immunohistochemistry and fluorescence in situ hybridization (FISH):* Mouse brains and spinal cords were fixed in 4% paraformaldehyde, pH 7.4, and embedded in paraffin. Four  $\mu\text{m}$  thick serial sections were cut and mounted onto positively charged microscope slides.

Antigen retrieval was performed by submerging the sections in citrate buffer (pH 6.0) and microwaved at 800 W for 10 min. For mouse monoclonal primary antibody (anti-ubiquitin, 1:500, Cat #MAB1510, Chemicon) the M.O.M. immunodetection kit (Cat. #BMK-2202, Vector Lab) was used according to recommended protocol and incubation with the antibody was performed overnight at 4°C in a humid chamber. For all other antibodies (anti-nucleolin: rabbit polyclonal, 1:1000, Cat #ab22758, Abcam; anti-p62: rabbit polyclonal, 1:500, Cat # BML-PW9860-0100, Enzo Life Sciences; and anti-N-terminal TDP-43: 1:4000, Cat # 10782-2-AP, Proteintech Group, Inc.) the sections were treated with 1% H<sub>2</sub>O<sub>2</sub>/Methanol and blocked with 10% horse serum followed by overnight incubation with the primary antibodies. The following fluorescent secondary antibodies from Molecular Probes were used (4h at room temperature) Alexa Fluor 488 (Cat. #A11034), Alexa Fluor 594 (Cat #A11037), Alexa Fluor 488 (Cat #A11029) or Alexa Fluor 594 (Cat #A11032). Nuclei were stained with DAPI and mounted with prolong gold antifade mountant. Positive and negative controls were run along each batch of sections processed.

For Poly(GP) immunohistochemistry five micron thick sagittal slices of mouse hemibrain were cut from formalin-fixed, paraffin-embedded blocks and mounted on glass slides. After drying, slides were deparaffinized and rehydrated in xylene and alcohol washes before being steamed for 30 min in 1X Tris-EDTA (pH 9) buffer solution for antigen retrieval. All slides were processed on a Dako Autostainer with the Dako EnVision™+ system and 3'3'-diaminobenzidine chromogen. After staining with anti-GP serum (1:10,000) (Ash et al., 2013), slides were counterstained with Lerner hematoxylin and coverslipped with Cytoseal permanent mounting media.

RNA FISH was performed as reported previously described (Sareen et al., 2013), with some modifications. Four  $\mu\text{m}$  serial tissue sections were deparaffinized using xylenes and hydrated with decreasing concentrations of ethanol and then permeabilized, washed, and incubated as previously reported. Sequences of the LNA oligonucleotide probes: sense probe: 5TYE563/CCCCGGCCCCGGCCCC and antisense probe: /5TYE563/GGGGCCGGGGCCGGGG (Product #500150, Exiqon Inc. Woburn, MA, USA).

When immunofluorescence was combined with RNA FISH, RNA FISH was performed as mentioned above up to the steps of post-hybridization washes and then the slides were blocked for 15 min with 10% horse serum in TBS/0.5% Triton X-100 and then incubated with primary antibody overnight at 4°C in a humid chamber. The following antibodies were used; anti-Pur-alpha (LifeSpan Biosciences, Cat #LS-B6784), anti-hnRNP H (Abcam, Cat #ab10374), anti-hnRNP A2/B1 (GeneTex, Cat # GTX117578), and anti- hnRNP A3 (Sigma, Cat #AV41195). As described above, secondary antibody were used at 1:1000 dilution for 30 min at room temperature, incubation with DAPI, and the slides were mounted with prolong gold antifade moutant. The stained sections were evaluated and photographed with an Olympus BX51 Upright Microscope.

*RNA isolation and real-time qRT-PCR and Western blot analysis:* RNA isolation was performed as previously described with minor changes (Sareen et al., 2013). Tissue was lysed using TRIzol<sup>®</sup> and a tissue grinder according to the protocol (Life Technologies). RNA (1  $\mu\text{g}$ ) was first deoxyribonuclease-treated and then reverse-transcribed to cDNA with either oligo(dT) or Random hexamers with the Promega Reverse Transcriptase System. qPCRs were performed in triplicate with SYBR Green Master Mix (Applied Biosystems). Human C9orf72 (Forward: 5'-

CAGTGATGTCGACTCTTTG-3' and Reverse: 5'-AGTAGCTGCTAATAAAGGTGATTTG-3') expression was normalized to mouse beta-actin (Forward: 5'-AGGTATCCTGACCCTGAAG-3' and Reverse: 5'-GCTCATTGTAGAAGGTGTGG-3') and 18S-5' (Forward: 5'-GCTCGCGCTTCCTTACCT-3' and Reverse 5'-GCGACCAAAGGAACCATAACTG-3'), 18S (Forward: 5'-GATGGTAGTCGCCGTGCC -3' and Reverse: 5'-GCCTGCTGCCTTCCTTGG-3'), 18S-3' (Forward:5'-CGTCGCTACTACCGATTGGA-3' and Reverse: 5'-CCCGTTTAATGATCCTTCCGC-3') 5.8S-5' (Forward: 5'-taccgatacgactcttagcggt-3' and Reverse: 5'-CGACGCTCAGACAGGCGTAG-3') 5.8S (Forward: 5'-GATCACTCGGCTCGTGCGT -3' and Reverse: 5'-CGACGCTCAGACAGGCGTAG -3'), and 28S (Forward: 5'-GAACTATGCTTGGGCAGGG -3' and Reverse: 5'-GTCTTTCGCCCCTATACCCA-3') was normalized to 45S (Forward: 5'-GGGCTGTGTGGTTGTGTC-3' and Reverse: 5'-GACACGGACCCTCTCGAC -3'). For Western blot analysis, tissue was lysed in cold RIPA buffer, and quantitated using BCA assay (Pierce). C9orf72 was detected with anti-C9orf72 (ProteinTech), and mouse beta-actin was detected with anti-actin (Sigma) along with fluorescent secondary antibodies and the Odyssey imager from LI-COR.

*RNA-seq and 5'-RACE analysis:* RNA was purified and sequencing libraries were generated for either Illumina (spinal cord) or IonTorrent (cortex) sequencing per manufacturer's instructions. The resulting reads were aligned to mouse genome build mm9 using TOPHAT. BAM files were imported to Partek software to generate RPKM values and for differential expression analysis. Gene Set Enrichment Analysis (GSEA) was performed following recommendations detailed on the GSEA website (Mootha et al., 2003; Subramanian et al., 2005) with 1000 permutations of the

gene sets and a false discovery rate p-value of less than 0.05 was accepted as significant. 5' rapid amplification of cDNA ends (5'-RACE) analysis was performed as previously described with the GeneRacer kit (Invitrogen, catalog no. L1502-02) according to the manufacturer's instructions, with modifications as noted previously (Sareen et al., 2013).

*Methylation assays of C9orf72 locus:* Genomic DNA was isolated using the Puregene Core A kit (Qiagen, Valencia, CA, USA) or the DNeasy Blood and Tissue Kit (Qiagen, Valencia, CA, USA). Quantitative assessment of *C9orf72* promoter methylation was assessed as described previously (Russ et al., 2015) where DNA was double digested with HaeIII and the methylation-sensitive HhaI, or single digested with HaeIII. Digested DNA was subject to qPCR to determine the difference in cycles to threshold amplification in order to calculate the percent methylation of the *C9orf72* promoter.

*C9RAN Immunoassay:* Post-mortem tissue from mice or human cases was subjected to a sequential protein extraction protocol as previously described (Almeida et al., 2013). In brief, tissues were lysed in RIPA buffer, sonicated, and centrifuged at 100,000 g for 30 min at 4 °C. The RIPA-insoluble pellet was then extracted using 7 M urea buffer, sonicated and centrifuged at 100,000 g for 30 min at 22 °C. Poly(GP) levels were measured using a previously described sandwich immunoassay that utilizes Meso Scale Discovery (MSD) electrochemiluminescence detection technology (Su et al., 2014). Serial dilutions of recombinant (GP)<sub>8</sub> in TBS were used to prepare the standard curve. Response values corresponding to the intensity of emitted light upon electrochemical stimulation of the assay plate using the MSD QUICKPLEX SQ120 were acquired. Responses from mouse and human samples were background corrected using the



average response from lysates obtained from non-transgenic mice or FTLD cases lacking the *C9orf72* expansion, respectively, prior to interpolation of poly(GP) levels using the standard curve. Poly(GP) protein expression in frontal cortical homogenates from 2 C9FTLD patients were used for comparison to C9-BAC mice.

*DPR immunoassay in primary cortical cultures:* Cells were lysed in buffer containing 50 mM Tris-HCl, pH 7.4, 300 mM NaCl, 1% Triton X-100, 2% sodium dodecyl sulfate, 5 mM EDTA, as well as protease (EMD Millipore, USA) and phosphatase inhibitors (Sigma-Aldrich, USA). After sonication, samples were centrifuged at 16,000 x g for 20 min at 4°C and supernatants collected. The protein concentration of lysates was determined by BCA assay (Thermo Scientific, USA). Poly(GP) levels in lysates were measured by sandwich immunoassay, as described above. Response values were background corrected using the average response from lysates obtained from primary cultures of non-transgenic mice prior to interpolation of poly(GP) levels.

*Human tissues:* Frozen frontal cortex tissues were obtained from the brain bank for neurodegenerative disorders at Mayo Clinic in Jacksonville, Florida, which operates under protocols approved by the Mayo Clinic Institutional Review Board, in accordance with Health Insurance Portability and Accountability Act guidelines.

*Mouse behavioral analysis:* For all behavioral tests, mice were acclimated to the testing room for a minimum of 60 minutes prior to each round of testing. *Rotarod:* Mice were placed on the stationary rod. Once all mice faced the back of the device, a constant speed of 4.0 rpm was

started followed by an acceleration of 0.1 rpm/sec over a five minute period. Latency to fall and behavior was recorded for each trial. A total of four trials were run with 10 minutes recovery time between each trial. If a subject fell with a latency of <5 seconds, it was given up to 3 attempts within each trial to 'try again.'

*Grip strength:* The Chatillon-Ametek Digital Force Gauge, DFIS 2 (Columbus Instruments, Columbus, OH) was used to determine the strength exerted by the forelimbs of an animal in response to a constant downward force. The grip strength meter was positioned vertically, with the triangular metal transducer situated 40 cm above a foam platform. Mice were lifted toward the triangular shaped force transducer, and a trained investigator monitors the mouse for instinctive grip reflex of both forepaws on the transducer; then firmly pulls the mouse straight down from the bar. Peak force was measured in kilograms (kg) for 5 consecutive trials and an average was calculated for each animal. Data presented as average of 5 trials as force in grams (g) and normalized to body weight (g/kg).

*Open field:* Versamax Open Field Arenas (40 cm x 40 cm x 40 cm) were used for this test. Lighting in the testing room is consistent with the housing room (~400-500 lux). Mice were placed individually into the center of the arena and infrared beams record distance traveled (cm), and perimeter/center time.

*Three-Chamber:* Mice were placed in the middle of a three-chamber arena divided into three equal compartments and the test was adapted from previously described protocols (Moy et al., 2004). The testing sessions consisted of a ten minutes habituation phase where the arena was empty and the test mouse could explore all three chambers, followed by a ten minutes sociability phase. The sociability phase consisted of a stranger mouse (male A/J mouse) placed within an enclosure on one side of the arena while, in the opposite side, only an enclosure was added, serving as novel object. Intact sociability was indicated by a significant preference of the test mouse for the chamber with the stranger vs. the chamber with the object,

while low sociability was indicated by a lack of preference for the stranger. Results in the form of the times spent in each chamber (object only, neutral, stranger mouse) were analyzed with a two-way ANOVA testing for the effects of the genotype and the chamber preference. *Y-Maze*: A clear Plexiglas Y-maze was used for this test under ambient lighting (~ 50 lux). Mice were placed midway of the start arm (A), facing the center of the y for an 8 minute test period and the sequence of entries into each arm are recorded via a ceiling mounted camera integrated with behavioral tracking software (Noldus Ethovision). % spontaneous alternation was calculated as the number of triads (entries into each of the 3 different arms of the maze in a sequence of 3 without returning to a previously visited arm) relative to the number of alteration opportunities.

*Peripheral axon counts and neuromuscular junction staining*: For peripheral axon counts, the sensory and motor branch of the femoral nerve were dissected above the medial quadriceps femoris and fixed in 2% glutaraldehyde, 2% paraformaldehyde, in 0.1 M cacodylate buffer overnight at 4 degrees. Both nerve branches were embedded in plastic and 0.5- $\mu$ m sections were cut and stained with toluidine blue. For axon counting and axon area measurement, images were captured using a Nikon Eclipse E600 microscope with a 40 objective. Automated quantification was performed as described in detail previously (Bogdanik et al., 2013). Briefly, with the ImageJ software, the Threshold function was used to highlight axoplasm only on whole nerve sections; the Analyze Particle function was then used to count the number of myelinated axons and their cross-sectional areas in each nerve. Counts and average areas were averaged for six 9-months old males per genotype.

Neuromuscular junction staining and imaging was performed as described before (Bogdanik et al., 2013). In brief, the tibialis anterior was dissected and fixed in cold 2% buffered

paraformaldehyde (prepared fresh) overnight. The muscle was embedded in 3% agarose in PBS and sectioned with a vibratome into 100- $\mu$ m thick sections. Sections were incubated overnight at room temperature in a cocktail of the primary antibodies anti-neurofilament 2H3 (PMID: 3272160) and anti-SV2 (PMID: 2579958) from the Developmental Studies Hybridoma Bank, each at a 1:250 dilution in PBS, 1% TritonX100, 1% BSA. Sections were washed and incubated overnight with an Alexa-Fluor-488 conjugated anti-mouse IgG1 and Alexa-Fluor-594 conjugated  $\alpha$ -bungarotoxin (Invitrogen), each at a 1:1000 dilution in the same buffer as above. Sections were mounted in fluorescence mounting medium (DAKO, S3023) and imaged on a Leica SP5 laser confocal microscope at 40x magnification.

*RNA foci and nucleolin quantification:* RNA foci CY3 images were subject to Nearest Neighbor processing and then merged with DAPI image. 5 random images from each brain region were blindly counted for both sense and antisense foci. Only nuclear RNA foci were counted. For the 6 month time point for sense and antisense counts included NTg (n= 4), F08-CTR (n=4), F112 (n=4). For the time course at 3 months n=4 (sense); n=3 (antisense), at 6 months n=4 (sense and antisense), and at 8 months n= 3 (sense and antisense). For nucleolin counts, 5 random images were obtained from 3 nontransgenic age-matched controls and 3 transgenic C9-BACexp (F112) at 8 months for each brain region. Nucleolin displacement was calculated using ImageJ software as follows (Total nucleolin – nucleolin in nucleolus/nuclear area- nucleolar area= nucleolin dispersed in the nucleus).

*Primary cortical neuron cultures, ASO treatments, calcium imaging, glutamate toxicity assay:*

Primary cortical neurons cultures were prepared from P1 pups and cultured in B27-Neurobasal medium for 14 days. To measure calcium activity, cultured cortical neurons were labeling with Fluo-4 Direct™ Calcium Assay Kit (Life Tech, #F10471) and recorded. Briefly, cortical cultures at 2 weeks were incubated with calcium indicator prepared according to manufacturer's instruction for 30 min at 37°C. Time-lapse images were captured every 30 seconds for 5 minutes on ImageXpress Micro XLS system and quantified on ImageXpress. To measure glutamate toxicity, cultured cortical neurons were exposed to increasing concentration of glutamate (0, 50mM, 500mM) for 24 hours. Toxicity was determined by calculating the percent of neurons (TuJ1) present after treatment. All images and cell counts were obtained using the ImageXpress. For antisense oligonucleotide treatments, cortical cultures derived from P10 pups were treated with RNase H dependent gapmer ASOs (control ASO - 141923 – CCTTCCCTGAAGGTTCTCC; Exon 2 ASO-576816 – GCCTTACTCTAGGACCAAGA targeting all isoforms of human *C9orf72*) for 14 days, and processed for either FISH or DPR immunoassay measurements.

*Statistical Analyses:* Grip Strength statistical analysis was determined by Student's t test. Rotarod was determined by two-way repeat measure ANOVA, with the Bonferroni correction for multiple tests. Open Field, Three-Chamber, Y-Maze, and Three-Chamber were analyzed by two-way ANOVA using the Bonferroni post hoc test. Axon counts were analyzed by ordinary one-way ANOVA. Nucleolin displacement was analyzed using Student's t test. All data are shown as mean ± SEM, and all analyses were conducted using Prism software (Graphpad).

## References

Almeida, S., Gascon, E., Tran, H., Chou, H.J., Gendron, T.F., Degroot, S., Tapper, A.R., Sellier, C., Charlet-Berguerand, N., Karydas, A., *et al.* (2013). Modeling key pathological features of frontotemporal dementia with C9ORF72 repeat expansion in iPSC-derived human neurons. *Acta Neuropathol* 126, 385-399.

Ash, P.E., Bieniek, K.F., Gendron, T.F., Caulfield, T., Lin, W.L., DeJesus-Hernandez, M., van Blitterswijk, M.M., Jansen-West, K., Paul, J.W., 3rd, Rademakers, R., *et al.* (2013). Unconventional Translation of C9ORF72 GGGGCC Expansion Generates Insoluble Polypeptides Specific to c9FTD/ALS. *Neuron* 77, 639-646.

Bogdanik, L.P., Sleight, J.N., Tian, C., Samuels, M.E., Bedard, K., Seburn, K.L., and Burgess, R.W. (2013). Loss of the E3 ubiquitin ligase LRSAM1 sensitizes peripheral axons to degeneration in a mouse model of Charcot-Marie-Tooth disease. *Disease models & mechanisms* 6, 780-792.

Mootha, V.K., Lindgren, C.M., Eriksson, K.F., Subramanian, A., Sihag, S., Lehar, J., Puigserver, P., Carlsson, E., Ridderstrale, M., Laurila, E., *et al.* (2003). PGC-1alpha-responsive genes involved in oxidative phosphorylation are coordinately downregulated in human diabetes. *Nat Genet* 34, 267-273.

Moy, S.S., Nadler, J.J., Perez, A., Barbaro, R.P., Johns, J.M., Magnuson, T.R., Piven, J., and Crawley, J.N. (2004). Sociability and preference for social novelty in five inbred strains: an approach to assess autistic-like behavior in mice. *Genes, brain, and behavior* 3, 287-302.

Russ, J., Liu, E.Y., Wu, K., Neal, D., Suh, E., Irwin, D.J., McMillan, C.T., Harms, M.B., Cairns, N.J., Wood, E.M., *et al.* (2015). Hypermethylation of repeat expanded C9orf72 is a clinical and molecular disease modifier. *Acta Neuropathol* 129, 39-52.

Sareen, D., O'Rourke, J.G., Meera, P., Muhammad, A.K., Grant, S., Simpkinson, M., Bell, S., Carmona, S., Ornelas, L., Sahabian, A., *et al.* (2013). Targeting RNA foci in iPSC-derived motor neurons from ALS patients with a C9ORF72 repeat expansion. *Science translational medicine* 5, 208ra149.

Su, Z., Zhang, Y., Gendron, T.F., Bauer, P.O., Chew, J., Yang, W.Y., Fostvedt, E., Jansen-West, K., Belzil, V.V., Desaro, P., *et al.* (2014). Discovery of a biomarker and lead small molecules to target r(GGGGCC)-associated defects in c9FTD/ALS. *Neuron* 83, 1043-1050.

Subramanian, A., Tamayo, P., Mootha, V.K., Mukherjee, S., Ebert, B.L., Gillette, M.A., Paulovich, A., Pomeroy, S.L., Golub, T.R., Lander, E.S., *et al.* (2005). Gene set enrichment analysis: a knowledge-based approach for interpreting genome-wide expression profiles. *Proc Natl Acad Sci U S A* 102, 15545-15550.